Molecular and Crystal Structures of *endo*- and *exo*-*N*-Methyl-3,7-epoxy-3-methoxy-7-oxo-1,2-benzo-1-cycloheptene-4,5-dicarboximide

Hatsue TAMURA, Toshikazu IBATA, and Kazuhide OGAWA*
College of General Education, Osaka University, Toyonaka, Osaka 560
(Received June 27, 1983)

The crystal structures of *endo*- and *exo*-adducts of 1-methoxy-2-benzopyrylium-4-olate with *N*-methylmaleimide have been determined by means of X-ray analysis. The colorless crystals of the *endo*-adduct are orthorhombic, with the space group $P2_12_12_1$ and with a=14.432(3), b=11.874(2), c=7.762(1) Å, and Z=4. The colorless crystals of the *exo*-adduct are monoclinic, with the space group $P2_1/a$ and with a=13.381(2), b=12.825(1), c=7.4793(4) Å, β=92.13(1)°, and Z=4. The structures were deduced by a direct method and refined by a block-diagonal least-squares technique. The final R values for the *endo*- and *exo*-adducts are 0.047 for 1160 observed reflections and 0.067 for 1986 observed reflections respectively. The configurations of the *endo*- and *exo*-adducts are coincident with those assigned on the basis of the NMR data. The observed values of the ring-current effect on the *N*-methyl chemical shift of the *endo*-adduct and the coupling constants of the vicinal methine protons of both adducts are in good agreement with the ones calculated on the basis of the present X-ray crystal-structure analysis.

The chemistry of carbonyl ylide has received the continuous interest of heterocyclic chemists for the past two decades.[1] One of the present authors (T. I.) has reported the novel formation of carbonyl ylide by the carbene-carbonyl reaction.[2] As an application of this reaction, the $Cu(acac)_2$-catalyzed decomposition of *o*-methoxycarbonyl-α-diazoacetophenone (**1**) was reported to give 1-methoxy-2-benzopyrylium-4-olate (**3**) as a transient species in a high yield *via* an intramolecular carbene-carbonyl reaction of intermediate keto carbene (**2**). The cycloaddition of the pyrylium-4-olate (**3**) to *N*-methylmaleimide gave two adducts: **4a**, mp 210°C; **4b**, 230°C.[3] The reaction procedure is shown in Scheme 1. The two adducts, **4a** and **4b**, were assigned to *endo*- and *exo*-cycloadducts respectively on the basis of their NMR data.[3] In order to confirm the assignment of the structures, an X-ray analysis of the adducts was carried out. Then, using the crystal data thus obtained, the ring-current effect and the coupling constants were calculated according to Farnum-Wilcox's method[4] and Williamson-John's equation[5] respectively.

Experimental

Colorless crystals of the *endo*- and *exo*-adducts were obtained from benzene solutions. The crystal data of the *endo*- and *exo*-adducts, along with the experimental conditions, are listed in Table 1. The X-ray intensity data were measured on a Rigaku four-circle diffractometer with Ni-filtered Cu $K\alpha$ radiation. The numbers of non-zero reflections used in the structure determination were 1160 for the *endo*- and 1986 for the *exo*-adduct. The intensities were corrected for Lorentz and polarization effects.

The NMR spectra of the *endo*- and *exo*-adducts were reexamined on a Hitachi NMR spectrometer, model FT-100, in $CDCl_3$, using TMS as the internal standard, to obtain accurate values of the chemical shifts and coupling constants.

Structure Determination. Using 170 reflections with $|E| \geq 1.39$ for the *endo*-adduct and 170 reflections with $|E| \geq 1.80$ for the *exo*-adduct, the crystal structures were determined by the direct method with the MULTAN 78 program.[6] The *E*-maps computed with the phase sets of the highest combined figure of merit (2.996 for the *endo*-adduct and 3.000 for the *exo*-adduct) revealed the positions of all the non-hydrogen atoms. Several cycles of block-diagonal least-squares refinement with isotropic temperature factors brought the R values to 0.096 for the *endo*-adduct and to 0.121 for the *exo*-adduct. The refinement with anisotropic temperature factors then reduced the R values to 0.061 for the *endo*-adduct and to 0.081 for the *exo*-adduct. At this stage, all the hydrogen atoms except those of the methyl groups were located by means of difference syntheses. After several cycles of block-diagonal least-squares refinement, the R values were reduced to 0.047 for the *endo*-adduct and to 0.067 for the *exo*-adduct. The function minimized was $\sum w(F_o - |F_c|)^2$ with the following weighting scheme: $w = 1/(\sigma(F_o)^2 + 0.0823|F_o| + 0.0013|F_o|^2)$ for the *endo*-adduct and $w = 1/(\sigma(F_o)^2 + 0.0783|F_o| + 0.0028|F_o|^2)$ for the *exo*-adduct.

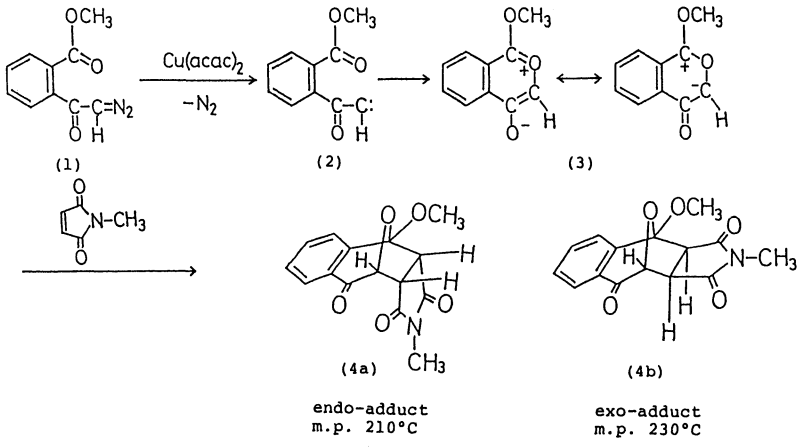

Scheme 1.

TABLE 1. CRYSTAL AND EXPERIMENTAL DATA

	endo-Adduct	*exo*-Adduct
Crystal system	Orthorhombic	Monoclinic
Space group	$P2_12_12_1$	$P2_1/a$
a	14.432(3) Å	13.381 (2) Å
b	11.874(2)	12.825(1)
c	7.762(1)	7.4793(4)
β		92.13(1)°
V	1330.1(3) Å^3	1282.6(2) Å^3
Z	4	4
D_m	1.439 Mg m^{-3}	1.485 Mg m^{-3}
D_x	1.435	1.488
μ(Cu $K\alpha$)	0.93 mm^{-1}	0.96 mm^{-1}
Scan method	θ-2θ	θ-2θ
Scan speed in ω	4°min^{-1}	4°min^{-1}
Scan width	1.2°+0.15° tanθ	1.2°+0.15° tanθ
Background	2×4 s	2×4 s
$2\theta_{max}$(Cu $K\alpha$)	120°	125°
No. of Reflections	1164	2326
	1160(except $\|F_o\|$=0)	1986(except $\|F_o\|$=0)
Crystal size	0.4×0.4×0.3 mm^3	0.2×0.2×0.1 mm^3

TABLE 2(a). ATOMIC POSITIONAL (×10^4) AND THERMAL PARAMETERS FOR *endo*-ADDUCT

Atom	x	y	z	B_{eq}/Å^2
O(1)	-239(1)	3497(1)	3769(3)	2.9
O(2)	-108(1)	1944(1)	2025(3)	3.2
O(3)	663(2)	4231(2)	7679(3)	5.0
O(4)	2380(1)	2145(2)	1427(3)	3.8
O(5)	2430(2)	5073(2)	5184(4)	4.8
N	2595(1)	3533(2)	3451(3)	2.7
C(1)	794(2)	1996(2)	4539(4)	2.7
C(2)	934(2)	2537(2)	6111(4)	2.9
C(3)	660(2)	3737(3)	6305(4)	3.2
C(4)	355(2)	4294(2)	4645(4)	3.0
C(5)	1169(2)	4464(2)	3335(4)	2.5
C(6)	1121(2)	3425(2)	2177(4)	2.3
C(7)	373(2)	2674(2)	3073(4)	2.6
C(8)	1078(2)	882(2)	4336(4)	3.3
C(9)	1495(2)	322(3)	5699(5)	4.1
C(10)	1633(2)	843(3)	7260(5)	4.8
C(11)	1363(3)	1980(3)	7483(4)	4.1
C(12)	2089(2)	2933(2)	2240(4)	2.4
C(13)	2122(2)	4432(2)	4117(4)	2.6
Me(14)	3541(2)	3216(3)	3938(5)	4.3
Me(15)	-690(3)	2462(3)	714(5)	4.4

TABLE 2(b). ATOMIC POSITIONAL (×10^4) AND THERMAL PARAMETERS FOR *exo*-ADDUCT

Atom	x	y	z	B_{eq}/Å^2
O(1)	6925(1)	-630(1)	4150(2)	2.4
O(2)	8161(1)	552(1)	4908(2)	2.8
O(3)	4572(1)	-476(2)	1986(3)	2.7
O(4)	9520(1)	107(2)	2040(3)	4.2
O(5)	7309(2)	-2341(2)	23(4)	5.0
N	8587(2)	-1265(2)	998(3)	2.9
C(1)	6533(2)	1187(2)	3822(3)	2.4
C(2)	5555(2)	900(2)	3294(3)	2.4
C(3)	5381(2)	-171(2)	2591(3)	2.7
C(4)	6297(2)	-859(2)	2621(3)	2.6
C(5)	6959(2)	-575(2)	1028(3)	2.7
C(6)	7690(2)	243(2)	1794(3)	2.5
C(7)	7355(2)	374(2)	3745(3)	2.3
C(8)	6728(2)	2212(2)	4341(4)	3.1
C(9)	5944(2)	2924(2)	4403(4)	3.7
C(10)	4967(2)	2627(2)	3918(4)	3.6
C(11)	4772(2)	1617(2)	3362(4)	3.1
C(12)	8720(2)	-267(2)	1669(3)	2.7
C(13)	7612(2)	-1508(2)	608(4)	3.2
Me(14)	9428(3)	-1977(3)	747(5)	4.3
Me(15)	7952(2)	524(3)	6795(4)	4.1

All the atomic scattering factors were taken from the "International Tables for X-Ray Crystallography."[7] The computations were carried out on an ACOS-S700 computer at the Crystallographic Research Center, Institute for Protein Research Laboratory, Osaka University, using "The Universal Crystallographic Computing System-Osaka."[8] Table 2 lists the final atomic and thermal parameters, along with their estimated standard deviations.[9] The bond distances and angles are given in Fig. 1.

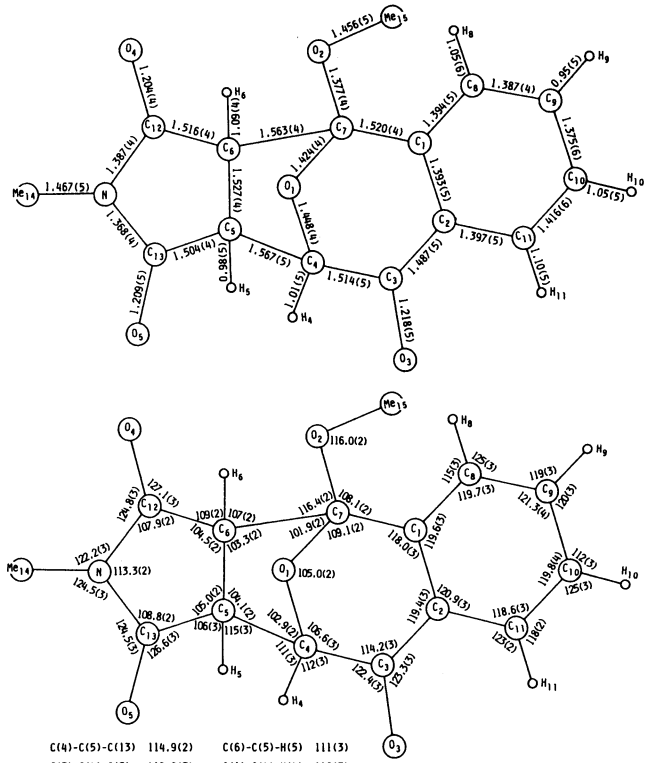

C(4)-C(5)-C(13)	114.9(2)	C(6)-C(5)-H(5)	111(3)
C(3)-C(4)-C(5)	112.9(3)	O(1)-C(4)-H(4)	110(3)
C(7)-C(6)-C(12)	113.7(2)	C(5)-C(6)-H(6)	119(2)
O(1)-C(7)-O(2)	110.0(2)	C(1)-C(7)-C(6)	111.0(2)

(a)

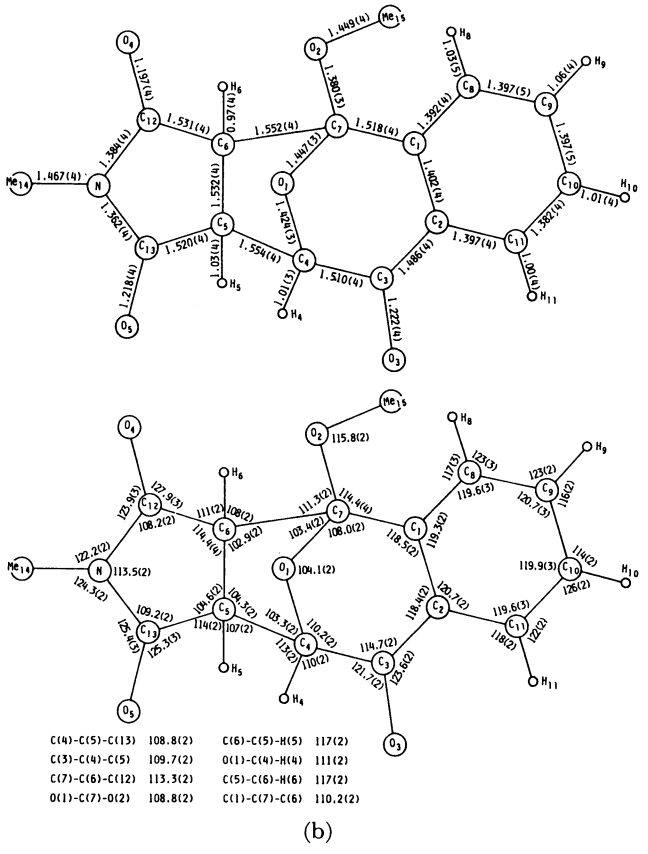

C(4)-C(5)-C(13)	108.8(2)	C(6)-C(5)-H(5)	117(2)
C(3)-C(4)-C(5)	109.7(2)	O(1)-C(4)-H(4)	111(2)
C(7)-C(6)-C(12)	113.3(2)	C(5)-C(6)-H(6)	117(2)
O(1)-C(7)-O(2)	108.8(2)	C(1)-C(7)-C(6)	110.2(2)

(b)

Fig. 1. (a) Bond distances and angles of the *endo*-adduct. (b) Bond distances and angles of the *exo*-adduct.

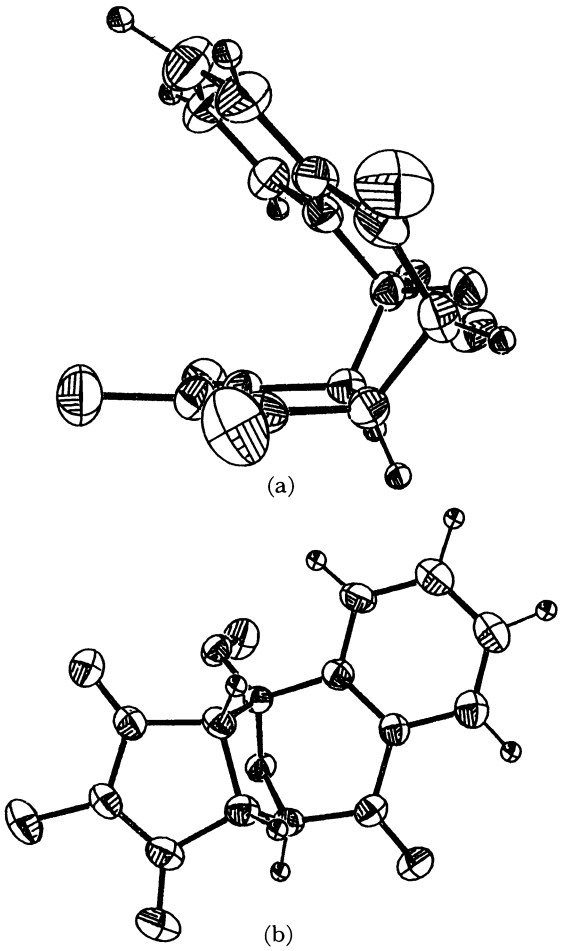

(a)

(b)

Fig. 2. (a) ORTEP view of the *endo*-adduct. (b) ORTEP view of the *exo*-adduct.
The non-hydrogen atoms were drawn at the 50% probability level and the hydrogen atoms were drawn with an arbitrary diameter.

Results and Discussion

Molecular Structure. The molecular structures of the *endo*- and *exo*-adducts are given in Figs. 2(a) and 2(b)[10] respectively. It was confirmed from these structures that the assignment of the configuration to these compounds deduced from the NMR data[3] was correct. The corresponding bond distances and angles in the *endo*- and *exo*-adducts agree fairly well with each other. As is shown in Fig. 1, the N–C, C–O, and C–C bond lengths in the succinimide ring system of both compounds are comparable to those in the derivatives of succinimide.[11–13] The bond lengths between the bridged oxygen atom(O(1)) and the bridgehead carbon atom (C(4) or C(7)) in both compounds are similar to those found in some oxygen-bridged ring compounds.[14] The difference between the O(1)–C(4) and O(1)–C(7) bond distances in the *endo*- or *exo*-adduct can be regarded as significant. The intramolecular distances between O(1) and Me(15) are shorter than the van der Waals' distance; that is, they are 2.749 Å in the *endo*-adduct and 2.792 Å in the *exo*-adduct.

The equations of the best planes through the four selected sets of atoms and the dihedral angles between

TABLE 3(a). BEST PLANES OF THE *endo*-ADDUCT

(a) Equations
The plane equations are of the $AX+BY+CZ+D=0$ form, where X,Y,Z, and D are measured in Å units: $X=ax$, $Y=by$, and $Z=cz$.
Plane(A): N, C(5), C(6), C(12), C(13)
$-0.3225X-0.5818Y+0.7466Z+1.6674=0$
Plane(B): C(4), C(5), C(6), C(7)
$-0.6729X+0.3996Y-0.6225Z+0.5711=0$
Plane(C): O(1), C(4), C(7)
$0.0769X+0.5346Y-0.8416Z+0.2691=0$
Plane(D): C(1), C(2), C(3), C(4), C(7)
$-0.9325X-0.2403Y+0.2694Z+0.6787=0$
(b) Dihedral angles(ϕ/°) between the planes:
(A)-(B) 241.3(or 118.7)
(B)-(C) 46.7
(C)-(D) 115.3
(B)-(D) 68.7

TABLE 3(b). BEST PLANES OF THE *exo*-ADDUCT

(a) Equations
The plane equations are of the $AX+BY+CZ+D=0$ form, where X,Y,Z, and D are measured in Å units: $X=ax+czcos\beta$, $Y=by$, and $Z=czsin\beta$.
Plane(A): N, C(5), C(6), C(12), C(13)
$-0.1331X-0.3575Y+0.9243Z+0.2541=0$
Plane(B): C(4), C(5), C(6), C(7)
$-0.6336X+0.7171Y-0.2902Z+6.6446=0$
Plane(C): O(1), C(4), C(7)
$-0.7805X+0.4560Y+0.4276Z+6.1845=0$
Plane(D): C(1), C(2), C(3), C(4), C(7)
$0.2170X+0.3004Y-0.9288Z+0.3338=0$
(b) Dihedral angles(ϕ/°) between the planes:
(A)-(B) 116.1(or 243.9)
(B)-(C) 45.8
(C)-(D) 115.4
(B)-(D) 69.7

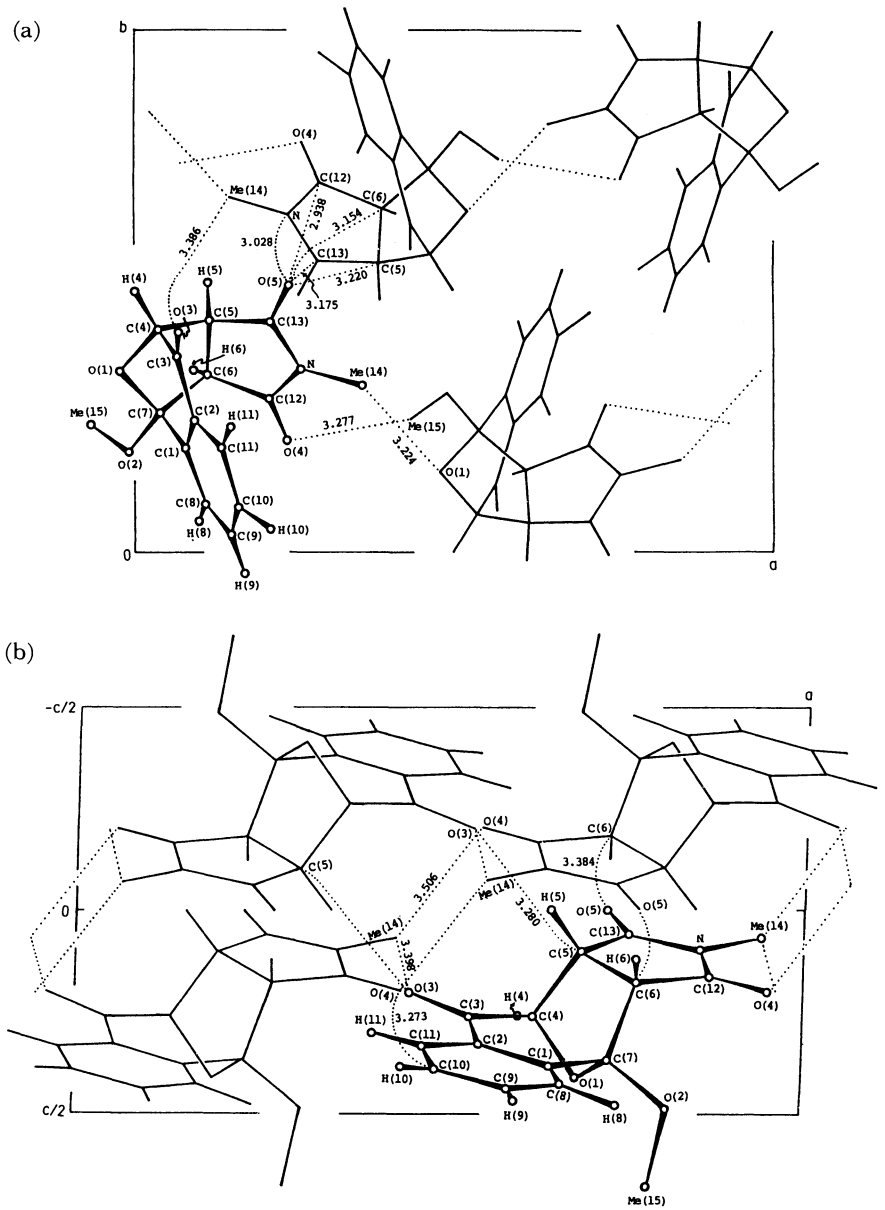

Fig. 3. (a) Crystal structure of the *endo*-adduct projected along the c axis. (b) Crystal structure of the *exo*-adduct projected along the b axis.

them are given in Table 3. The differences between the dihedral angles in the *endo*-adduct and the corresponding ones in the *exo*-adduct are not regarded as significant, but the dihedral angle between the plane (A) and the plane (B) of the *endo*-adduct is opposite to that of the *exo*-adduct in sign, that is, direction. The five-membered ring of the succinimide moiety is planar, with all deviations within ±0.04 Å in the *endo*-adduct and within ±0.02 Å in the *exo*-adduct. The C(3) and O(3) atoms deviate from the plane of the benzene ring by 0.033 Å and by −0.111 Å respectively in the *endo*-adduct, while they deviate by 0.106 and 0.225 Å in the *exo*-adduct.

Crystal Structure. The crystal structure of the *endo*-adduct projected along the c axis is shown in Fig. 3(a) and that of the *exo*-adduct projected along the b axis in Fig. 3(b). Some of the shorter intermolecular contacts are shown by dotted lines.

Ring-current Effect. The ring-current effect on chemical shifts and the values of the coupling constants are usually calculated using the Johnson-Bovey equation[15] and the Karplus equation[16] respectively. However, almost all the present calculations have been based on the values obtained by an inspection of such models as the CPK model or the Dreiding model. In this respect, the molecular model based on the atomic coordinates determined by X-ray analysis is expected to make possible a better interpretation of the NMR data and afford solider grounds for those equations than the above-mentioned models.

The *endo*-adduct showed its *N*-CH_3 signal at 2.37 ppm, and the *exo*-adduct, at 3.08 ppm, which was similar to the value of *N*-methylsuccinimide (2.98 ppm). This high-field shift of the *endo*-adduct by 0.71 ppm was attributed to the ring-current effect by the benzene ring located close to the *N*-CH_3 group. The values of 3.18 as *Z* and 0.50 as ρ in Farnum-Wilcox's double-torus model[4] were derived from the molecular structure found in the present X-ray work, as is shown in Fig. 4. The value of the ring-current effect of the *endo*-adduct was estimated from the "isoshielding" lines of the Johnson-Bovey ring-current effect by the use of the values of *Z* and ρ obtained above. This calculated value (0.85 ppm) is close to the experimental one (0.71 ppm).

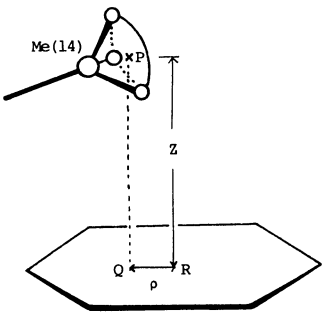

Fig. 4. Configuration of the methyl group (Me(14)) and the benzene ring in the calculation of the ring current effect of the *endo*-adduct.
P: The center of the triangle of the hydrogen atoms, Q: the foot of perpendicular line from P to the plane of the benzene ring, R: the center of the benzene ring. Tetrahedral structure and the C–H bond length of 1.08 Å are assumed for Me(14) radical. The parameters, *Z* and ρ, which are used for the estimation of the ring current effect, can be obtained as shown in the figure.

TABLE 4. OBSERVED AND CALCULATED VALUES OF VICINAL COUPLING CONSTANTS

		$J_{5,6}$/Hz	$J_{4,5}$/Hz
endo-Adduct	Obsd	9.5	9.2
	Calcd[a]	9.5	9.1
exo-Adduct	Obsd	7.5	0.0
	Calcd[a]	10.0	0.0

a) Williamson-Johnson's equation:

$$J_{HH} = \begin{cases} 10\cos^2\phi & (0° \leq \phi \leq 90°) \\ 16\cos^2\phi & (90° \leq \phi \leq 180°). \end{cases}$$

Coupling Constant. The observed coupling constants, $J_{5,6}$ and $J_{4,5}$, of both adducts are listed in Table 4. The coupling constants of the vicinal protons depend mainly on the dihedral angle, and they can be calculated by the Karplus method.[16] Of the several modified Karplus equations thus far reported, Williamson-Johnson's equation[5] was found to be most suitable for the ring system in this work. According to the present X-ray crystal-structure analysis, the dihedral angles between the C(5)–C(6)–H(6) plane and the C(6)–C(5)–H(5) plane, and between the C(5)–C(4)–H(4) plane and the C(4)–C(5)–H(5) plane, in the *endo*-adduct were found to be 13° and 17° respectively, while the corresponding dihedral angles in the *exo*-adduct were found to be 1° and 89°. The coupling constants calculated by substituting these dihedral angles (ϕ) in Williamson-Johnson's equation[5] are also shown in Table 4. These calculated values are in good agreement with the observed values obtained on the basis of the NMR spectra.

References

1) R. Huisgen, *Angew. Chem., Int. Ed. Engl.*, **1977**, 572.
2) K. Ueda, T. Ibata, and M. Takebayashi, *Bull. Chem. Soc. Jpn.*, **45**, 2779 (1972).
3) T. Ibata, K. Jitsuhiro, and Y. Tsubokura, *Bull. Chem. Soc. Jpn.*, **54**, 240 (1981).
4) D. G. Farnum, *J. Am. Chem. Soc.*, **89**, 2970 (1967); D. G. Farnum and C. F. Wilcox, *ibid.*, **89**, 5379 (1967).
5) K. L. Williamson and W. S. Johnson, *J. Am. Chem. Soc.*, **83**, 4623 (1961).
6) P. Main, S. E. Hull, L. Lessinger, G. Germain, J-P. Declercq, and M. M. Woolfson, "A System of Computer Programs for the Automatic Solution of Crystal Structures from X-ray Diffraction Data," MULTAN 78, University of York (1978).
7) "International Tables for X-Ray Crystallography," Kynoch Press, Birmingham (1974), Vol. IV, p. 71.
8) T. Ashida, "The Universal Crystallographic Computing System-Osaka, HBLS V," The Computation Center, Osaka University (1979), p. 53; T. Ashida, "The Universal Crystallographic Computing System-Osaka, DAPH," The Computation Center, Osaka University (1979), p. 61.
9) The F_O and F_C tables, anisotropic temperature factors, and hydrogen positional and isotropic thermal parameters are kept as Document No. 8408 at the Chemical Society of

Japan.
10) C. K. Johnson, "ORTEP-II: A FORTRAN Thermal-Ellipsoid Plot Program for Crystal-structure Illustrations, ORNL-5138," March, 1976, Oak Ridge National Laboratory.
11) A. Kirfel, *Acta Crystallogr., Sect.B*, **32**, 1556 (1976).
12) R. Mason, *Acta Crystallogr.*, **14**, 720 (1961).
13) R. N. Brown, *Acta Crystallogr.*, **14**, 711 (1961).
14) E. O. Schlemper, T. Shinmyozu, and J. P. McCormick, *Acta Crystallogr., Sect. B*, **38**, 2981 (1982); B. Berking and N. C. Seeman, *ibid.*, **27**, 1752 (1971); Olga Kennard and D. G. Watson, *ibid.*, **26**, 1038 (1970); E. B. Fleischer and T. S. Srivastava, *ibid., Sect.A*, **25**, S195 (1969); Young Ja Park, H. S. Kim, and G. A. Jeffrey, *ibid., Sect. B*, **27**, 220 (1971); Isabella L. Karle, *ibid.*, **31**, 1519 (1975).
15) C. E. Johnson, Jr., and F. A. Bovey, *J. Chem. Phys.*, **29**, 1012 (1958).
16) M. Karplus, *J. Chem. Phys.*, **30**, 11 (1959).